

# SAPK: A Novel Composite Resin for Water Treatment with Very High $\text{Zn}^{2+}$ , $\text{Cd}^{2+}$ , and $\text{Pb}^{2+}$ Adsorption Capacity

Emmanuel I. Unuabonah,<sup>\*,†,‡</sup> Bamidele I. Olu-Owolabi,<sup>§,||</sup> Andreas Taubert,<sup>‡</sup> Elizabeth B. Omolehin,<sup>§</sup> and Kayode O. Adebawale<sup>§</sup>

<sup>†</sup>Department of Chemical Sciences, Redeemer's University, 110115 Mowe, Nigeria

<sup>‡</sup>Institute of Chemistry, University of Potsdam, D-14476 Potsdam, Germany

<sup>§</sup>Department of Chemistry, University of Ibadan, 200284 Ibadan, Nigeria

<sup>||</sup>Institut für Bodenkunde und Bodenerhaltung, Universität Gießen, 35392 Gießen, Germany

## Supporting Information

**ABSTRACT:** A new sulfonated aniline-modified poly(vinyl alcohol)/K-feldspar (SAPK) composite was prepared. The cation-exchange capacity of the composite was found to be 5 times that of neat feldspar. The specific surface area and point of zero charge also changed significantly upon modification, from  $15.6 \pm 0.1 \text{ m}^2/\text{g}$  and 2.20 (K-feldspar) to  $73.6 \pm 0.3 \text{ m}^2/\text{g}$  and 1.91 (SAPK).  $\text{Zn}^{2+}$ ,  $\text{Cd}^{2+}$ , and  $\text{Pb}^{2+}$  adsorption was found to be largely independent of pH, and the metal adsorption rate on SAPK was higher than that on neat feldspar. This particularly applies to the initial adsorption rates. The adsorption process involves both film and pore diffusion; film diffusion initially controls the adsorption. The Freundlich and Langmuir models were found to fit metal-ion adsorption on SAPK most accurately. Adsorption on neat feldspar was best fitted with a Langmuir model, indicating the formation of adsorbate monolayers. Both pure feldspar and SAPK showed better selectivity for  $\text{Pb}^{2+}$  than for  $\text{Cd}^{2+}$  or  $\text{Zn}^{2+}$ .

## ■ INTRODUCTION

High concentrations of heavy-metal ions in the aquatic environment are an immense threat for public health, especially in developing countries.<sup>1–3</sup> Heavy metals are nonbiodegradable, cumulative poisons that cause severe physiological damage.<sup>1,4,5</sup> For example, cadmium causes lung and kidney damage, bone diseases, gastrointestinal and renal dysfunction, and cancer.<sup>4,6–10</sup> Lead poisoning particularly affects young children, who can absorb up to 50% of the lead they ingest.<sup>1,4,11</sup> Once ingested through the gastrointestinal track, lead accumulates in vital organs such as kidneys, liver, and brain. It binds to thiol and phosphate groups in proteins, nucleic acids, and cell membranes,<sup>12</sup> resulting in severe neurological and/or hematological disfunction.<sup>11,13</sup> Efficient, selective, and inexpensive water adsorbents are therefore among the top priorities for improving public health in developing countries.

Indeed, large amounts of data are available on different organic materials,<sup>14,15</sup> as well as clay minerals<sup>16–39</sup> and polymer/clay composites,<sup>20,40–42</sup> for metal-ion removal from aqueous solution. Clay is a popular adsorbent, because different clays easily exchange ions with the environment and, thus, efficiently remove heavy metals from water.<sup>14,39,43,44</sup> Moreover, they can easily be modified with polymers that aid sorption.<sup>42</sup> In contrast, there are virtually no studies on feldspar-based adsorbents.<sup>45–47</sup> This is intriguing because feldspar is the single most abundant mineral group on Earth.<sup>48</sup> As feldspar is thus easily available and inexpensive, it would, in principle, also be a viable adsorbent for water purification. Obviously, the chemistries of clay minerals and feldspar are different, and it is therefore not straightforward to translate findings from clay-based adsorbents to feldspar-based materials. New approaches for feldspar-based adsorbents are thus needed.

The current article therefore discusses the preparation, characterization, and application of a novel sulfonated aniline-modified poly(vinyl alcohol) (PVA)/feldspar composite resin (SAPK) for the efficient removal of  $\text{Pb}^{2+}$ ,  $\text{Cd}^{2+}$ , and  $\text{Zn}^{2+}$  from aqueous solution. Reacting feldspar first with PVA increases its stability in water for easy recovery from aqueous suspension. At the same time, the composite retains the ability to interact with cationic adsorbates (such as metal ions) in solution.<sup>32</sup> Sulfonic acid groups were introduced to increase the cation-exchange capability of the composite adsorbent, even under very acidic conditions where most adsorbents become inefficient.<sup>49</sup>

## ■ EXPERIMENTAL SECTION

**Materials.** Feldspar was obtained from Federal Industrial Research Oshodi (FIRO), Lagos State, Nigeria. The sample was treated as described previously.<sup>50</sup> Analar grades of poly(vinyl alcohol) (PVA, 87% hydrolyzed, 78 kg/mol, Merck); aniline, nitric acid, and sulfuric acid (BDH Chemicals), and nitrate salts of  $\text{Pb}^{2+}$ ,  $\text{Cd}^{2+}$ , and  $\text{Zn}^{2+}$  [ $\text{Pb}(\text{NO}_3)_2$ , 99%;  $\text{Cd}(\text{NO}_3)_2 \cdot 4\text{H}_2\text{O}$ , 98.5%;  $\text{Zn}(\text{NO}_3)_2 \cdot 6\text{H}_2\text{O}$ , 99.9%; (BDH Chemicals) were used as received.

**Modification of Feldspar.** PVA/feldspar was prepared according to the method of Unuabonah et al.<sup>51</sup> For the preparation of SAPK, 30 mL of aniline was added to 300 mL of 0.1 M  $\text{HNO}_3$  under stirring. To this solution was added 60 g of PVA/feldspar. After being stirred for 6 h at room temperature, the sample was washed several times with deionized water and

**Received:** September 12, 2012

**Revised:** November 28, 2012

**Accepted:** December 3, 2012

**Published:** December 3, 2012

dried at 348 K. The composite was subsequently sulfonated using 10 g of aniline/PVA/feldspar in 100 mL of 2 M  $\text{H}_2\text{SO}_4$ . The mixture was refluxed for 6 h, washed several times with 200 mL of deionized water, and dried at 573 K. This material is subsequently referred to as sulfonated aniline-modified PVA/K-feldspar composite resin (SAPK). The details of SAPK formation are not entirely clear at the moment, but we presume that the PVA stabilizes the feldspar microcrystals. As PVA swells in water, the aniline molecules can penetrate the PVA surface coating of the particles and, as the modification with aniline is done in the presence of  $\text{HNO}_3$ , adsorb on the negatively charged feldspar surface through the protonated amino group of the aniline. The aromatic ring of the aniline is subsequently sulfonated by treatment with sulfuric acid.

**Characterization.** Fourier transform infrared (FTIR) spectra were obtained on a Shimadzu 8400S FTIR spectrometer operated in transmission mode from 4000 to 400  $\text{cm}^{-1}$ . KBr pellets were produced using a Shimadzu MHP-1 mini hand press. X-ray diffraction patterns were recorded on a Siemens D-5000 instrument from  $1.5^\circ$  to  $50^\circ$  ( $2\theta$ ) at  $0.02^\circ \text{ s}^{-1}$ . Scanning electron microscopy was performed on a Philips XL30 instrument equipped with an EDAX energy-dispersive X-ray spectrometer. Particle size analysis was performed with a Beckman Coulter LS 230 laser granulometer counter. Thermal analysis [thermogravimetry (TG), differential thermogravimetry (DTG), differential thermal analysis (DTA)] was performed on a Netzsch 409 PC simultaneous thermal analyzer under a  $\text{N}_2$  flow ( $100 \text{ mL min}^{-1}$ ) at a heating rate of  $10^\circ \text{ C min}^{-1}$ . X-ray fluorescence (XRF) data were acquired on a Bruker AXS S4 Pioneer XRF spectrometer with analysis range from Be to U. Elemental analysis was performed on an Elementar vario EL III instrument. Point-of-zero-charge (PZC) determination was performed according to the method of Kinniburgh et al.<sup>52</sup> Specific surface areas (SSAs) were determined using the method of Sears.<sup>53</sup> Cation-exchange capacities (CECs) were determined using the ammonium acetate method of Chapman.<sup>54</sup> Atomic absorption spectroscopy (AAS) was performed on a Perkin-Elmer Analyst 800 high-performance atomic absorption spectrometer, and pH measurements were performed on a Hanna Bench pH Meter with calibration buffers at pH 4.0 and 7.0.

#### Metal-Ion Adsorption Studies: General Procedure.

One gram of unmodified feldspar or 0.5 g of SAPK was weighed into polyethylene bottles. Then, 20 mL of metal nitrate solution (50 mg/L) was added to each bottle. The samples were agitated for 5 h at room temperature. After agitation, the suspensions were centrifuged at 1500 rpm for 15 min, and the supernatants were analyzed by AAS. AAS control experiments with solutions containing only the metal ions (no adsorbent) were performed for comparison.

**Effect of pH.** The reaction was performed as described for the general procedure, but the pH values of the suspensions were adjusted between  $3.0 \pm 0.2$  and  $7.0 \pm 0.2$  using 0.1 M NaOH or HCl.

**Effect of Adsorbent Dose.** The reaction was performed as described for the general procedure, but various amounts (0.1, 0.2, 0.5, 0.7, 1.0 g) of feldspar or SAPK were used. Based on the results obtained from the pH studies (see Results and Discussion for details), the initial solution pH was  $6.0 \pm 0.2$  for unmodified feldspar and  $5.5 \pm 0.2$  for SAPK.

**Effect of Initial Metal-Ion Concentration.** The reaction was performed as described for the general procedure, but the metal concentrations were varied between 5 and 100 mg/L. Based on

the results obtained from the pH studies (see Results and Discussion for details), the initial solution pH was  $6.0 \pm 0.2$  for unmodified feldspar and  $5.5 \pm 0.2$  for SAPK.

**Effect of Time (Sorption Kinetics).** The reaction was conducted as described for the general procedure, and aliquots were collected at various times from 0 to 300 min. Based on the results obtained from the pH studies (see Results and Discussion for details), the initial solution pH was  $6.0 \pm 0.2$  for unmodified feldspar and  $5.5 \pm 0.2$  for SAPK.

The amounts of metal ions adsorbed by the adsorbents were calculated by difference using the equation

$$q_e = \frac{(C_0 - C_e)V}{w} \quad (1)$$

where  $q_e$  is the amount of metal ion adsorbed (mg/g),  $C_0$  is the initial metal-ion concentration (mg/L),  $C_e$  is the equilibrium concentration of metal ion in solution (mg/L),  $V$  is the volume of aqueous solution (L), and  $w$  is the weight of adsorbent (g).

**Data Fitting and Modeling.** Equilibrium sorption data were fitted to the Freundlich,<sup>55</sup> Langmuir,<sup>56</sup> Redlich–Peterson,<sup>57</sup> Fritz–Schlunder three-parameter,<sup>58</sup> and Fritz–Schlunder four-parameter<sup>58</sup> equilibrium models.<sup>59</sup> Kinetic data were fitted to pseudo-first-order, pseudo-second-order, diffusion–chemisorption,<sup>60,61</sup> and intraparticle diffusion<sup>62</sup> models. All data analysis was done with the Excel Solver add-in software using the nonlinear regression mode. Details of the models, equations, and analysis can be found in the Supporting Information.

The small-sample corrected Akaike information criterion (AICc) statistical tool was used in ranking these models for their reliability.<sup>63</sup> The AICc is a methodology for model selection in a situation where more than one model has been fitted to experimental data and the most appropriate model is to be identified.<sup>64,65</sup> It shows its strength in ranking even closely fitted models. The general form for calculating the AICc is given as

$$\text{AICc} = \text{AIC} + \left[ \frac{2k(k+1)}{n-k-1} \right] \quad (2)$$

where  $k$  is the number of parameters in the model,  $n$  is the number of data points, and  $\text{AIC} = 2k - 2 \ln(L)$ .<sup>63</sup> (The variable  $L$  is the maximized value of the likelihood function for the estimated model.) The model for which AICc is a minimum describes the experimental data best. To find out how much a model is better than others in describing a set of experimental data, the Akaike weight descriptor  $\lambda_i$  is used (see the Supporting Information for details). This approach allows not only for the identification of the best model, but also for the ranking of the models according to their appropriateness for the problem at hand.<sup>66,67</sup>

## RESULTS AND DISCUSSION

**Materials.** FTIR spectroscopy (data not shown) yielded only fairly nondescript spectra with broad and overlapping features. The data, therefore, did not allow for the identification of the sulfonate groups, mainly because the respective signals overlap with the Si–OH and Al–O signals. Nevertheless, elemental analysis (EA) found 1.33% N and 0.13% S in SAPK. This indicates that both the modification with aniline and the subsequent sulfonation were successful, although at fairly low levels.

Figure 1 shows thermogravimetric analysis (TGA) data for pure feldspar, aniline-modified PVA/feldspar, and SAPK. Pure

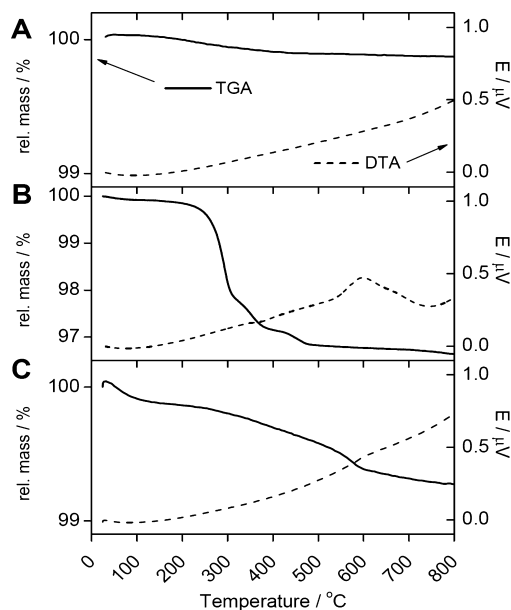


**Figure 1.** TGA and DTA data for (A) neat feldspar, (B) aniline-modified PVA feldspar, and (C) SAPK. Note that the y axis in panel B has a different scale than those in panels A and C.

feldspar shows no significant weight loss as a function of temperature. In contrast, (nonsulfonated) aniline-modified PVA/feldspar shows three transitions. It loses ca. 2% of its weight between 200 and 380 °C, <1% between 400 and 520 °C, and <0.5% between 520 and 610 °C. These losses can be assigned to loss of structural water and heat-induced condensation reactions, similar to those observed, for example, in silica.<sup>68,69</sup>

After sulfonation, TGA of SAPK shows a weight loss of <0.5% already at ca. 100 °C followed by a second, broad weight loss between ca. 200 and 800 °C. The first weight loss is due to removal of adsorbed water. The second loss can be assigned to the decomposition of the organic residues in SAPK. This smaller weight loss in SAPK compared to the aniline-modified composite could be due to sulfonic acid-induced stabilization of the composite.<sup>70,71</sup> Alternatively, the reduction in organic matter could be due to the fact that the sulfonation process already leads to the degradation of some organic material.

Differential thermal analysis (DTA) shows that, in the case of pure feldspar and SAPK, no significant exothermic or endothermic transitions occur. In contrast, the DTA curves of aniline-modified PVA feldspar, the precursor of SAPK, show an endothermic signal at ca. 600 °C followed by an exothermic signal at ca. 750 °C. This indicates that, in this material, a thermally induced decomposition of the organic material takes place.<sup>72</sup> Presumably, in the other two cases, the organic fraction is simply too low for observation of these signals.

X-ray diffraction (XRD) analysis of the raw mineral shows that it is a feldspar containing microcline and quartz (Figure 2). This suggests that the feldspar in this study was a mixture of two minerals: K-feldspar (F) and microcline (M), a feldspar variety that is closely related to K-feldspar. The reflections at 20.08° (2θ) (3.83 Å, 201) and 27.80° (2θ) (2.89 Å, 040) can be assigned to microcline and feldspar minerals, respectively. The reflections at 25.6° (2θ) (3.11 Å, 002) and 30.44° (2θ) (2.67 Å,

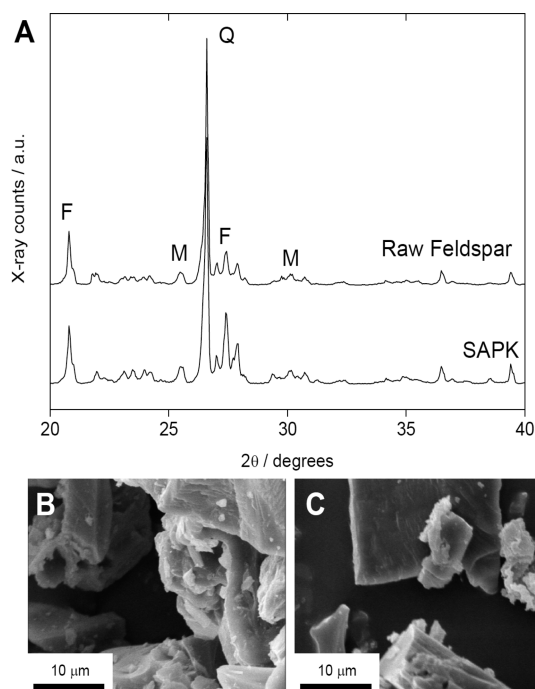


**Figure 2.** (A) X-ray diffraction patterns of the feldspar raw material and SAPK. (B,C) SEM images of (B) feldspar and (C) SAPK. F = K-feldspar, M = microcline, Q = quartz. For full XRD patterns, see Figure S1 (Supporting Information).

131) indicate that the crystals of the feldspar sample used in this study were partly monoclinic and partly triclinic.<sup>73</sup> The reflection at 26.60° (2θ) is from quartz (3.00 Å, 131), which was also present in the raw material. XRD clearly shows that the treatment with PVA, aniline, and sulfonic acid did not change the crystal structure or any *d* spacing, confirming that the treatment left the crystal structure of the feldspar starting material intact. The full X-ray diffraction patterns are shown in Figure S1 (Supporting Information).

Scanning electron microscopy (SEM) supports the XRD results, as there was no significant morphological difference between the neat feldspar and SAPK. Both samples consisted of particles with sharp angular shapes with smooth and relatively flat facets, which is typical of feldspars.

X-ray fluorescence (XRF; Table S1, Supporting Information) detected only a small change in the Si/Al ratio before (5.73) and after functionalization (5.93). XRF did, however, detect 0.23% sulfur in SAPK, but none in the original feldspar. This corroborates the EA results, which suggested that the SAPK samples were modified, but only at low levels. Measurements of the cation-exchange capacity (CEC) and the specific surface area (SSA) support the XRF, EA, and TGA findings in that they detected clear differences between the pure feldspar and SAPK. The SSA increased from 15.56 ± 0.1 to 73.6 ± 0.3 m<sup>2</sup>/g. It must be noted here, however, that the method used in this study (Sear's method)<sup>53</sup> quantifies –OH groups on a surface. These data are therefore indicative of the amount of hydroxyl groups per surface area and are not to be confused with surface areas obtained from gas sorption experiments. Finally, the CEC increased from 3.70 ± 0.2 to 25.43 ± 0.2 mequiv/100 g upon functionalization, and the point of zero charge (PZC) decreased from 2.20 to 1.91, similarly to earlier studies,<sup>51,74</sup> which further confirms a successful chemical modification.



Overall, XRD and SEM suggest that the reaction product was essentially identical to the feldspar starting material. XRF, CEC, SSA, PZC, and EA nevertheless show that functionalization of the feldspar with PVA and sulfonated aniline, although weak, did occur. The low degree of modification is not surprising because feldspar (the mineral detected by XRD, Figure 2) are tectosilicates. There are thus no pores or interlayers that could take up much organic material. Modification can therefore happen only on the small surface area available. Nevertheless, SAPK was found to be a much more efficient adsorbent for heavy metals than the feldspar raw material, as demonstrated by adsorption studies.

**Adsorption Properties. Equilibrium Studies. Effect of pH.** pH was found to have a stronger effect on the adsorption capacity of unmodified feldspar than on that of SAPK (Figure 3). This was most pronounced in the case of  $\text{Pb}^{2+}$ , for which

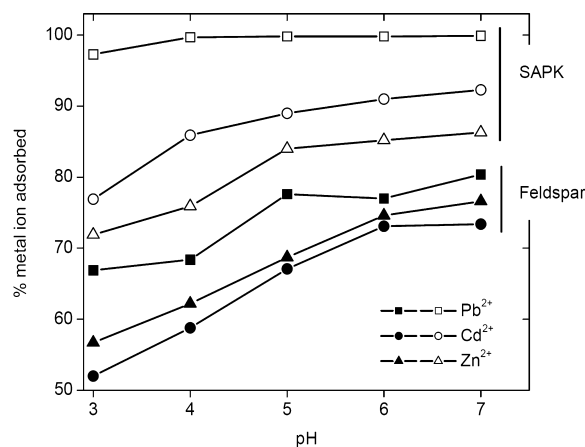


**Figure 3.** Effect of pH on  $\text{Zn}^{2+}$ ,  $\text{Cd}^{2+}$ , and  $\text{Pb}^{2+}$  adsorption on feldspar and SAPK.

the sorption capacity remained essentially the same throughout the entire pH range investigated. Overall, the capacity to adsorb metal ions from aqueous solutions at pH values as low as 3 increased from >50% (feldspar) to >70% in SAPK despite the low degree of functionalization. The effect was particularly pronounced for  $\text{Pb}^{2+}$ , where the adsorption reached close to 100% at pH values of 4 and higher.

**Effect of Adsorbent Dose.** Figure 4 shows the effect of adsorbent dose on the adsorption capacities of raw feldspar and SAPK. Increasing dosages of both adsorbents resulted in a decreasing equilibrium adsorption capacity,  $q_e$ . In contrast, the percentage of adsorbed metal ions increased with increasing adsorbent dose, similarly to previous studies.<sup>75,76</sup> This result is possibly due to a higher number of net negative charges (as more adsorbent was present in the suspension) and, correspondingly, a shorter-ranged electrostatic potential near the solid surface that favors adsorbent–adsorbate interaction. The decrease in  $q_e$  with increasing dosages might be due to aggregation of adsorbent particles at higher adsorbent doses, resulting in a decreasing total surface area and, correspondingly, an increasing diffusion path length, similarly to earlier data.<sup>76</sup>

AICc evaluation of the different adsorption models [see the Experimental Section for details and Tables S2 and S3 (Supporting Information) for AICc values for feldspar and SAPK] showed that the equilibrium adsorption data can best be fitted with a Langmuir isotherm;<sup>56,60</sup> see Table 1 for optimized parameters. Overall, the data confirm that SAPK is a better

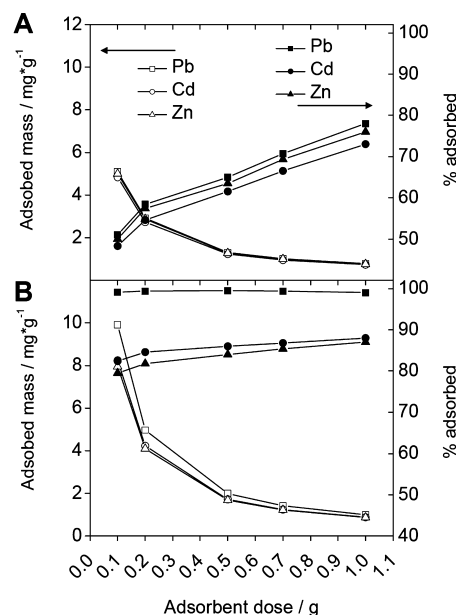


**Figure 4.** Effect of adsorbent dose on  $\text{Pb}^{2+}$ ,  $\text{Cd}^{2+}$ , and  $\text{Zn}^{2+}$  adsorption: (A) neat feldspar and (B) SAPK.

**Table 1.** Equilibrium Data for Feldspar and SAPK from Fitting to the Langmuir Isotherm

|          | $q_m$ ( $\text{mg g}^{-1}$ ) | $b$ ( $\text{L g}^{-1}$ ) | $r^2$  |
|----------|------------------------------|---------------------------|--------|
| Feldspar |                              |                           |        |
| Zn       | 1.62                         | 0.06                      | 0.9911 |
| Cd       | 1.67                         | 0.05                      | 0.9845 |
| Pb       | 1.69                         | 0.07                      | 0.9958 |
| SAPK     |                              |                           |        |
| Zn       | 5.97                         | 0.06                      | 0.9705 |
| Cd       | 5.58                         | 0.07                      | 0.9730 |
| Pb       | 6.82                         | 7.54                      | 0.9894 |

adsorbent for all of the metals investigated than the unmodified feldspar. In both cases (feldspar and SAPK), the preference for  $\text{Pb}^{2+}$  was found to be higher than that for  $\text{Cd}^{2+}$  or  $\text{Zn}^{2+}$ .

**Effect of Initial Metal-Ion Concentration.** Table 1 ( $q_e$  values) indicates that SAPK has approximately 5 times the adsorption capacity of feldspar for the removal of  $\text{Pb}^{2+}$ ,  $\text{Cd}^{2+}$ , and  $\text{Zn}^{2+}$  from aqueous solution. This also applies when the adsorption capacity of SAPK (this study) is compared to that of Na-feldspar.<sup>46</sup> From 100 mg/L solutions of  $\text{Zn}^{2+}$ , SAPK adsorbs 80%, whereas Na-feldspar adsorbs only ca. 39%.

AICc evaluation (Tables S2 and S3, Supporting Information) shows that the simpler Freundlich<sup>55</sup> and Langmuir<sup>56</sup> models give better fits to the experimental data than the models with more than two parameters, as can be seen from their lower relative Akaike weights  $\lambda_i$  compared to those of the other models. Adsorption on feldspar was found to be best fitted with the Langmuir model, whereas adsorption on SAPK was best fitted with the Langmuir ( $\text{Pb}^{2+}$  and  $\text{Cd}^{2+}$ ) and Freundlich ( $\text{Zn}^{2+}$ ) models.

Similar observations were made by Akpa and Unuabonah<sup>63</sup> and El-Khaiary and Malash.<sup>77</sup> In all cases, this suggests that feldspar has only one type of adsorption site with rather uniform surface energies. In contrast, SAPK has at least two types of adsorption sites, which is consistent with the concept of adsorption on both the free sites of the feldspar itself and the sulfonate groups of the aniline moieties. Moreover, as the

Langmuir and Freundlich models are essentially (sub)-monolayer models, the fact that the data can best be fitted with these isotherms suggests that the ions at most form a monolayer on the sorbent surfaces.

**Kinetic Studies.** Kinetic data were fitted with the nonlinear forms of three two-parameter kinetic models: (i) pseudo-first-order, (ii) pseudo-second-order, and (iii) diffusion–chemisorption kinetic models (see the Supporting Information for details).<sup>60,78</sup> AICc analysis (Table S4, Supporting Information) showed that, on feldspar, Zn<sup>2+</sup> adsorption is best fitted with the diffusion–chemisorption model, Pb<sup>2+</sup> adsorption with the pseudo-second-order kinetic model, and Cd<sup>2+</sup> adsorption with the pseudo-first-order model. On SAPK, Zn<sup>2+</sup> and Cd<sup>2+</sup> adsorption is best fitted with the pseudo-second-order model, and Pb<sup>2+</sup> adsorption is best fitted with the diffusion–chemisorption model.

These results suggest that both diffusion and chemisorption mechanisms are responsible for the adsorption of all metal ions on feldspar and SAPK. This conclusion is supported by the theories of the pseudo-second-order<sup>79</sup> and diffusion–chemisorption<sup>80</sup> models, with the exception of Cd<sup>2+</sup> adsorption on feldspar. This process is apparently controlled by mass transfer, as implied by the principles of the pseudo-first-order kinetic model.<sup>60,78,81</sup>

Table 2 shows that the modified feldspar minerals exhibited a better adsorption capacity ( $q_e$ ), initial adsorption rate ( $h$ ), and

**Table 2. Pseudo-Second-Order Kinetic Model Data for Feldspar and SAPK**

|          | $q_e$ (mg g <sup>-1</sup> ) | $k$ (g mg <sup>-1</sup> min) | $h$ (mg g <sup>-1</sup> min <sup>-1</sup> ) | $r^2$  |
|----------|-----------------------------|------------------------------|---|--------|
| Feldspar |                             |                              |   |        |
| Zn       | 0.76                        | 1.01                         | 0.58  | 0.9999 |
| Cd       | 0.73                        | 0.43                         | 0.22  | 0.9988 |
| Pb       | 0.78                        | 1.05                         | 0.65  | 1.0000 |
| SAPK     |                             |                              |   |        |
| Zn       | 1.70                        | 0.32                         | 0.93  | 0.9999 |
| Cd       | 1.74                        | 0.30                         | 0.90  | 0.9990 |
| Pb       | 1.99                        | 1.86                         | 7.44  | 1.0000 |

overall pseudo-second-order adsorption rate ( $k$ ) than the unmodified feldspar. Adsorption of Pb<sup>2+</sup> onto SAPK was highest, at 1.99 mg/g of SAPK adsorbent. This is close to 100% from solutions with  $C_{0,Pb(II)} = 50$  mg/L and roughly twice the amount adsorbed on neat feldspar. (Note that this should not be confused with the *equilibrium* adsorption results presented in the preceding section. In that case, the capacity of SAPK was found to be ca. 5 times larger than that of neat feldspar.) In 5 min, 97% adsorption of 50 mg/L Pb<sup>2+</sup> was achieved with SAPK (Figure S2a, Supporting Information).

Modification of feldspar to SAPK thus enhanced the *initial* adsorption rates for all metal ions. However, the *overall* pseudo-second-order kinetic rates for adsorption on SAPK were found to be lower than those for pure feldspar. This might be due to the increased adsorption capacity of SAPK, which could extend the equilibrium time. A notable exception is the overall pseudo-second-order kinetic rate for the adsorption of Pb<sup>2+</sup>, which might be due to the high selectivity of SAPK for this metal ion. Pb<sup>2+</sup> has the highest atomic weight, the highest electronegativity, and the highest standard reduction potential of the three elements studied here. This could play a role in the preference of SAPK for Pb<sup>2+</sup>, although the specifics are unclear at the moment.<sup>10</sup> This conclusion is further supported by the notion that Pb<sup>2+</sup> is a borderline acid, whereas Cd<sup>2+</sup> and Zn<sup>2+</sup> are soft acids. In accordance with Pearson's hard and soft acids and bases principle,<sup>82,83</sup> one can expect different interactions of hard, soft, and borderline bases with the different sorbents. Moreover, from the frontier molecular orbital (FMO) theory,<sup>84</sup> borderline (Lewis) acids such as Pb<sup>2+</sup> have intermediate properties and will therefore bind to both hard and soft (Lewis) bases (for example, the sulfonate groups of SAPK) through strong ionic interactions.

**Intraparticle Studies.** The film diffusion coefficients,  $D_1$ , for different initial metal-ion concentrations as calculated from the slope of the plots of  $q_t/q_e$  versus  $t$  (eq 23, Supporting Information) are reported in Table 3.  $Bt$  can then be calculated from eq 27 (Supporting Information) for different initial metal-ion concentrations. A plot of  $Bt$  versus  $t$  enables the determination of whether external transport or intraparticle diffusion controls the rate of adsorption. The plots were found to be linear at the initial period of adsorption and did not pass through the origin but rather cut the  $y$  axis between 1.9046 and 1.9145 (feldspar) and between 3.5997 and 1.6416 (SAPK). This indicates that external mass transfer is the rate-limiting process at the beginning of the adsorption process. Similarly, the pore diffusion coefficient  $D_2$  can be calculated from eq 28 (Supporting Information).

Table 3 lists the results for  $D_1$  and  $D_2$ . The data indicate that pore diffusion was faster than film diffusion and decreased with modification of the feldspar, similarly to the data reported by Onal et al.<sup>85</sup> In the current data set, the intercept approached zero with initial metal-ion concentration. This indicates an increasing influence of external mass transfer with increasing initial concentration. The decrease in  $D_2$  with modification to SAPK can possibly be explained by a decreasing number of free feldspar surface sites after modification with PVA. This further confirms our earlier suggestion that the mechanism of adsorption of Pb<sup>2+</sup>, Cd<sup>2+</sup>, and Zn<sup>2+</sup> onto both modified and unmodified feldspar adsorbents is a combination of diffusion and chemisorption.

**Table 3. Intraparticle Diffusion Data for Feldspar and SAPK**

|          | $D_1$ (cm <sup>2</sup> s <sup>-1</sup> ) | $r^2$  | intercept | $r^2$  | $D_2$ (cm <sup>2</sup> s <sup>-1</sup> ) | $k_{in}$ (mg g <sup>-1</sup> min <sup>-0.5</sup> ) | $r^2$  |
|----------|--|--------|-----------|--------|--|--|--------|
| Feldspar |  |        |           |        |  |  |        |
| Pb       | $2.22 \times 10^{-8}$                    | 0.8098 | 1.9046    | 0.9058 | $2.53 \times 10^{-6}$                    | $6.40 \times 10^{-3}$                              | 0.8098 |
| Cd       | $4.12 \times 10^{-4}$                    | 0.9915 | 1.2505    | 0.9052 | $2.19 \times 10^{-6}$                    | 1.65   | 0.9999 |
| Zn       | $1.27 \times 10^{-8}$                    | 0.9140 | 1.9145    | 0.9007 | $2.81 \times 10^{-6}$                    | $4.70 \times 10^{-3}$                              | 0.9140 |
| SAPK     |  |        |           |        |  |  |        |
| Pb       | $1.90 \times 10^{-10}$                   | 0.7295 | 3.5997    | 0.7039 | $3.56 \times 10^{-7}$                    | $3.10 \times 10^{-3}$                              | 0.7925 |
| Cd       | $2.48 \times 10^{-4}$                    | 0.9926 | 1.4719    | 0.9922 | $6.27 \times 10^{-8}$                    | 3.39   | 0.8856 |
| Zn       | $5.24 \times 10^{-9}$                    | 0.9499 | 1.6416    | 0.9710 | $5.46 \times 10^{-8}$                    | $1.43 \times 10^{-2}$                              | 0.9499 |

## SUMMARY AND CONCLUSIONS

Feldspar was modified with sulfonated aniline to produce a new sulfonated aniline-modified PVA/K-feldspar (SAPK) composite adsorbent. SEM and XRD (Figure 3) showed that the crystal structure of the inorganic starting material, K-feldspar, was not affected by the modification process. TGA, DTA (Figures 1 and 2), EA, SSA, PZC, and CEC along with extended sorption studies showed that the chemical modification was successful, but only on the surface of the feldspar.

Despite the low degree of modification, the functionalization was found to (i) increase the equilibrium adsorption capacity of feldspar to approximately 5 times its original capacity, (ii) reduce the PZC from 2.20 to 1.91, (iii) increase the CEC from 3.70 to 25.43 mequiv/100 g, and (iv) increase the specific surface area (number of surface hydroxyl groups) from 15.6 to 73.6 m<sup>2</sup>/g upon chemical modification. Importantly, SAPK exhibited better initial sorption rates for the adsorption of Pb<sup>2+</sup>, Cd<sup>2+</sup>, and Zn<sup>2+</sup> than the unmodified feldspar. Pore diffusion was found to be faster than film diffusion. Moreover, both feldspar and SAPK showed better selectivity for Pb<sup>2+</sup> than for Cd<sup>2+</sup> or Zn<sup>2+</sup>.

It was pointed out in the Introduction that feldspar-based sorbents could be very interesting for water remediation. The current report is among the first<sup>45–47</sup> on the topic and shows that successful modification into an efficient adsorbent for heavy metals is indeed possible. Although the degree of organic functionalization was rather low, the data clearly show that the concept is viable and should thus pave the way for further development of new water remediation tools in the developing countries. The diffusion data obtained in this study are, for example, the basis for the prediction of breakthrough curves in fixed-bed reactors, which could find application in the industrial treatment of water.

## ASSOCIATED CONTENT

### Supporting Information

Discussions of the various equilibrium and kinetic models used in this article. XRD patterns of neat and modified Feldspar (Figure S1), complete X-ray fluorescence data for feldspar and SAPK (Table S1), AICc values for various equilibrium isotherm models for metal-concentration-dependent equilibrium adsorption (feldspar, Table S2; SAPK, Table S3), AICc data for kinetic models; dashes indicate models that are not applicable to the data (Table S4). This material is available free of charge via the Internet at <http://pubs.acs.org>.

## AUTHOR INFORMATION

### Corresponding Author

\*E-mail: [iyaemma@yahoo.com](mailto:iyaemma@yahoo.com).

### Notes

The authors declare no competing financial interest.

## ACKNOWLEDGMENTS

We thank M. Junginger and R. Löbbicke for help in the laboratory and Dr. B. Hannemann for help with EA. E.I.U. acknowledges a Georg Forster Fellowship (Alexander von Humboldt Foundation). The University of Potsdam and the Alexander von Humboldt Foundation are thanked for financial support.

## REFERENCES

- (1) Goyer, R. A. *Handbook on Toxicity of Inorganic Compounds*; Marcel Dekker: New York, 1988.
- (2) Mandal, B. K.; Suzuki, K. T. Arsenic around the world: A review. *Talanta* **2002**, *58*, 201–235.
- (3) Denkhaus, E.; Salnikow, K. Nickel essentiality, toxicity, and carcinogenicity. *Crit. Rev. Oncol. Hematol.* **2002**, *42*, 35–56.
- (4) Walker, S. P.; Wachs, T. D.; Gardner, J. M.; Lozoff, B.; Wasserman, G. A.; Pollitt, E.; Carter, J. A.; International Child Development Steering Group. Child development: Risk factors for adverse outcomes in developing countries. *Lancet* **2007**, *369*, 145–157.
- (5) Choi, S. M.; Yoo, S. D.; Lee, B. M. Toxicological characteristics of endocrine-disrupting chemicals: Developmental toxicity, carcinogenicity, and mutagenicity. *J. Toxicol. Environ. Health B* **2004**, *7*, 1–32.
- (6) Jarup, L.; Akesson, A. Current status of cadmium as an environmental health problem. *Toxicol. Appl. Pharmacol.* **2009**, *238*, 201–208.
- (7) Loganathan, P.; Vigneswaran, S.; Kandasamy, J.; Naidu, R. Cadmium sorption and desorption in soils—A review. *Crit. Rev. Environ. Sci. Technol.* **2012**, *42*, 489–533.
- (8) Thompson, J.; Bannigan, J. Cadmium: Toxic effects on the reproductive system and the embryo. *Reprod. Toxicol.* **2008**, *25*, 304–315.
- (9) Wagner, G. J. Accumulation of cadmium in crop plants and its consequences to human health. *Adv. Agron.* **1993**, *51*, 173–212.
- (10) Ferreiros-Martinez, R.; Esteban-Gomez, D.; de Blas, A.; Platas-Iglesias, C.; Rodriguez-Blas, T. Eight-Coordinate Zn(II), Cd(II), and Pb(II) Complexes Based on a 1,7-Diaza-12-crown-4 Platform Endowed with a Remarkable Selectivity over Ca(II). *Inorg. Chem.* **2009**, *48*, 11821–11831.
- (11) Florea, A. M.; Busselberg, D. Occurrence, use and potential toxic effects of metals and metal compounds. *Biomaterials* **2006**, *19*, 419–427.
- (12) Sigel, H.; Da Costa, C. P.; Martin, R. B. Interactions of Lead(II) with Nucleotides and Their Constituents. *Coord. Chem. Rev.* **2001**, *219–221*, 435–461.
- (13) Castellino, N.; Castellino, P.; Sannolo, N., Eds. *Inorganic Lead Exposures: Metabolism and Intoxication*; Lewis: Boca Raton, FL, 1994.
- (14) Babel, S.; Kurniawan, T. A. Low-cost adsorbents for heavy metals uptake from contaminated water: A review. *J. Hazard. Mater.* **2003**, *97*, 219–243.
- (15) Ngah, W. S. W.; Teong, L. C.; Hanafiah, M. Adsorption of Dyes and Heavy Metal Ions by Chitosan Composites: A Review. *Carbohydr. Polym.* **2011**, *83*, 1446–1456.
- (16) Dubey, S. P.; Gopal, K.; Bersillon, J. L. Utility of adsorbents in the purification of drinking water: A review of characterization, efficiency and safety evaluation of various adsorbents. *J. Environ. Biol.* **2009**, *30*, 327–332.
- (17) El-Eswed, B.; Yousef, R. I.; Alshaar, M.; Khalili, F.; Khoury, H. Alkali solid-state conversion of kaolin and zeolite to effective adsorbents for removal of lead from aqueous solution. *Desalin. Water Treat.* **2009**, *8*, 124–130.
- (18) Park, Y.; Ayoko, G. A.; Frost, R. L. Application of organoclays for the adsorption of recalcitrant organic molecules from aqueous media. *J. Colloid Interface Sci.* **2011**, *354*, 292–305.
- (19) Sanchez, A. G.; Ayuso, E. A.; De Blas, O. J. Sorption of heavy metals from industrial waste water by low-cost mineral silicates. *Clay Miner.* **1999**, *34*, 469–477.
- (20) Srinivasan, R. Advances in Application of Natural Clay and Its Composites in Removal of Biological, Organic, and Inorganic Contaminants from Drinking Water. *Adv. Mater. Sci. Eng.* **2011**, *2011*, 872531.
- (21) Wang, L. X.; Li, J. C.; Jiang, Q.; Zhao, L. J. Water-soluble Fe<sub>3</sub>O<sub>4</sub> nanoparticles with high solubility for removal of heavy-metal ions from waste water. *Dalton Trans.* **2012**, *41*, 4544–4551.
- (22) Yang, L. Q.; Li, Y. F.; Hu, H. Y.; Jin, X. L.; Ye, Z. F.; Ma, Y. X.; Zhang, S. D. Preparation of novel spherical PVA/ATP composites with macroreticular structure and their adsorption behaviour for



methylene blue and lead in aqueous solution. *Chem. Eng. J.* **2011**, *173*, 446–455.

(23) Potgieter, J. H.; Potgieter-Vermaaka, S. S.; Kalibantonga, P. D. Heavy metals removal from solution by palygorskite clay. *Miner. Eng.* **2006**, *19*, 463–470.

(24) Chen, H.; Wang, A. J. Kinetic and isothermal studies of lead ion adsorption onto palygorskite clay. *Colloid Interface Sci.* **2007**, *307*, 309–316.

(25) Fan, Q.; Li, Z.; Zhao, H.; Jia, Z.; Xu, J.; Wu, W. Adsorption of Pb(II) on palygorskite from aqueous solution: Effects of pH, ionic strength and temperature. *Appl. Clay Sci.* **2009**, *45*, 111–116.

(26) Bhattacharyya, K. G.; Gupta, S. S. Adsorption of some heavy metal ions on sulfate- and phosphate-modified kaolin. *Adsorption* **2006**, *12*, 185–204.

(27) Srivastava, P.; Singh, B.; Angove, M. Competitive adsorption behavior of heavy metals on kaolinite. *J. Colloid Interface Sci.* **2005**, *290*, 28–38.

(28) Jiang, M.; Jin, X.; Lu, X.; Chen, Z. Adsorption of Pb(II), Cd(II), Ni(II) and Cu(II) onto natural kaolinite clay. *Desalination* **2010**, *252*, 33–39.

(29) Abollino, O.; Giacomino, A.; Malandrino, M.; Mentasti, E. Interaction, Interaction of metal ions with montmorillonite and vermiculite. *Appl. Clay Sci.* **2008**, *28*, 227–236.

(30) Ilic, M.; González, J.; Pohlmeier, A.; Narres, H. D.; Schwuger, M. J. Interaction of sodium dodecylsulfate (SDS) with homoionic montmorillonites: Adsorption isotherms and metal-ion release. *Colloid Polym. Sci.* **1996**, *274*, 966–973.

(31) Liu, Y.; Wu, P.; Dang, Z.; Ye, D. Heavy Metal Removal from Water by Adsorption Using Pillared Montmorillonite. *Acta Geologica Sinica* **2006**, *80*, 219–225.

(32) Doğan, M.; Turhan, Y.; Alkan, M.; Namli, H.; Turan, P.; Demirbaş, Ö. Functionalized sepiolite for heavy metal ions adsorption. *Desalination* **2008**, *230*, 248–268.

(33) Brigatti, M. F.; Frigieri, P.; Gardinali, C.; Medici, L.; Poppi, L.; Franchini, G. Treatment of industrial wastewater using zeolite and sepiolite, natural microporous materials. *Can. J. Chem. Eng.* **1999**, *77*, 163–168.

(34) Demirbaş, Ö.; Alkan, M.; Doğan, M.; Turhan, Y.; Namli, H.; Turan, P. Electrokinetic and adsorption properties of sepiolite modified by 3-aminopropyltriethoxysilane. *J. Hazard. Mater.* **2007**, *149*, 650–656.

(35) Guimarães, A. M. F.; Ciminelli, V. S. T.; Vasconcelos, W. L. Smectite organofunctionalized with thiol groups for adsorption of heavy metal ions. *Appl. Clay Sci.* **2009**, *42*, 410–414.

(36) Kubilay, S.; Gürkan, R.; Savran, A.; Şahan, T. Removal of Cu(II), Zn(II) and Co(II) ions from aqueous solutions by adsorption onto natural bentonite. *Adsorption* **2007**, *13*, 41–51.

(37) Olu-Owolabi, B. I.; Unuabonah, E. I. Adsorption of Zn<sup>2+</sup> and Cu<sup>2+</sup> onto sulphate and phosphate-modified bentonite. *Appl. Clay Sci.* **2011**, *51*, 170–173.

(38) Naseem, R.; Tahir, S. S. Removal of Pb(II) from Aqueous/Acidic Solutions by Using Bentonite as an Adsorbent. *Water Res.* **2001**, *35*, 3982–3986.

(39) Celis, R.; Hermosin, M. C.; Cornejo, J. Heavy metal adsorption by functionalized clays. *Environ. Sci. Technol.* **2000**, *34*, 4593–4599.

(40) Hwu, J. M.; Jiang, G. J.; Gao, Z. M.; Xie, W.; Pan, W. P. The Characterization of Organic Modified Clay and Clay-Filled PMMA Nanocomposite. *J. Appl. Polym. Sci.* **2002**, *83*, 1702–1710.

(41) Zhao, Q.; Samulski, E. T. A comparative study of poly(methyl methacrylate) and polystyrene/clay nanocomposites prepared in supercritical carbon dioxide. *Polymer* **2006**, *47*, 663–671.

(42) Liu, P. Polymer Modified clay minerals: A review. *Appl. Clay Sci.* **2007**, *38*, 64–76.

(43) Bhattacharyya, K. G.; Sen Gupta, S. Adsorption of a few heavy metals on natural and modified kaolinite and montmorillonite: A review. *Adv. Colloid Interface Sci.* **2008**, *140*, 114–131.

(44) Gatica, J. M.; Vidal, H. Non-cordierite clay-based structured materials for environmental applications. *J. Hazard. Mater.* **2010**, *181*, 9–18.

(45) Singh, D. B.; Rupainwar, D. C.; Prasad, G. Studies on the removal of Cr(VI) from waste-water by feldspar. *J. Chem. Technol. Biotechnol.* **1992**, *53*, 127–131.

(46) Asçe, Y.; Nurbas, M.; Açıkel, Y. S. Removal of zinc ions from a soil component Na-feldspar by a rhamnolipid biosurfactant. *Desalination* **2008**, *223*, 361–365.

(47) Al-Rawajfeh, A. E.; Al-Whoosh, K.; Al Dwairi, R.; Al-Maaberah, A.; Tarawneh, A. Pre-treatment of desalination feed seawater by Jordanian tripoli, pozzolana, and feldspar: Batch experiments. *Chem. Ind. Chem. Eng. Q.* **2011**, *17*, 163.

(48) Ribbe, P. H., Ed. *Feldspar Mineralogy*, 2nd ed.; Reviews in Mineralogy; Mineralogical Society of America: Chantilly, VA, 1983; Vol. 2.

(49) Krishnan, K. A.; Anirudhan, T. S. Removal of cadmium(II) from solutions by steam-activated sulphurized carbon prepared from sugar-cane bagasse pith. Kinetic and equilibrium studies. *Water SA* **2003**, *29*, 147–156.

(50) Adebawale, K. O.; Unuabonah, E. I.; Olu-Owolabi, B. I. Adsorption of some heavy metal ions on sulphate and phosphate-modified kaolin. *Appl. Clay Sci.* **2005**, *29*, 145–148.

(51) Unuabonah, E. I.; Olu-Owolabi, B. I.; Adebawale, K. O.; Yang, L. Z. Removal of lead and cadmium from aqueous solution by polyvinyl alcohol-modified kaolinite clay: A novel nanoclay adsorbent. *Adsorpt. Sci. Technol.* **2008**, *26*, 383–405.

(52) Kinniburgh, D. G.; Jackson, M. L.; Syers, J. K. Adsorption of alkaline earth, transition and heavy metal cations by hydrous oxide gels of Fe and Al. *Soil Sci. Soc. Am. J.* **1976**, *40*, 796–779.

(53) Sears, G. W. Determination of Specific Surface Area of Colloidal Silica by Titration with Sodium Hydroxide. *Anal. Chem.* **1956**, *28*, 1981–1983.

(54) Chapman, A. D. In *Methods of Soil Analysis*; American Society of Agronomy: Madison, WI, 1965; p 891.

(55) Freundlich, H. M. F. Over the adsorption in solution. *J. Phys. Chem.* **1906**, *57*, 385–471.

(56) Langmuir, I. The constitution and fundamental properties of solids and liquids. *J. Am. Chem. Soc.* **1916**, *38*, 2221–2295.

(57) Redlich, O.; Peterson, D. L. A useful adsorption isotherm. *J. Phys. Chem.* **1959**, *63*, 1024–1026.

(58) Fritz, W.; Schlunder, E. U. Simultaneous adsorption equilibria of organic solutes in dilute aqueous solution on activated carbon. *Chem. Eng. Sci.* **1974**, *29*, 1279–1282.

(59) Do, D. D. *Adsorption Analysis: Equilibria and Kinetics*; Imperial College Press: London, 1998.

(60) Yiacoumi, S.; Tien, C. *Kinetics of Metal Adsorption from Aqueous Solutions: Models, Algorithms, and Applications*; Springer: New York, 1995.

(61) Sutherland, C.; Venkobachar, C. A diffusion–chemisorption kinetic model for simulating biosorption using *Forest macro-fungus, Fomes fasciatus*. *Int. Res. J. Plant Sci* **2010**, *1*, 107–117.

(62) Crank, J. *The Mathematics of Diffusion*; 2nd ed.; Oxford University Press: New York, 1975.

(63) Akpa, O. M.; Unuabonah, E. I. Small-sample corrected Akaike information criterion: An appropriate statistical tool for ranking of adsorption isotherm models. *Desalination* **2011**, *272*, 20–26.

(64) Akaike, H. A new look at the statistical model identification. *IEEE Trans. Autom. Control* **1974**, *19*, 716–723.

(65) Burnham, K. P.; Anderson, D. R. Multimodal inference: Understanding AIC and BIC in model selection. *Sociol. Methods Res.* **2004**, *33*, 261–304.

(66) Bozdoğan, H. Information Criterion and Recent Developments in Information Complexity. *J. Math. Psychol.* **2009**, *44*, 62–91.

(67) Boyd, G. E.; Schubert, J.; Adamson, A. W. The exchange adsorption of ions from aqueous solutions by organic zeolites. I. Ion-exchange equilibria. *J. Am. Chem. Soc.* **1947**, *69*, 2818–2829.

(68) Göbel, R.; Friedrich, A.; Taubert, A. Tuning the Phase Behavior of Ionic Liquids in Organically Functionalized Silica Ionogels. *Dalton Trans.* **2010**, 603–611.

(69) Göbel, R.; Hesemann, P.; Weber, J.; Möller, E.; Friedrich, A.; Beuermann, S.; Taubert, A. Surprisingly High, Bulk-like Mobility of

Silica-confined Ionic Liquids. *Phys. Chem. Chem. Phys.* **2009**, *11*, 3653–3662.

(70) Santos, A. L. S.; Dias, M. L.; Antonelli, D. Structure and thermal properties of naphthalene sulfonated resin/mesoporous niobium oxide nanostructured composites. *Chem. Chem. Technol.* **2009**, *3*, 177–182.

(71) Wu, X.; He, G.; Gu, S.; Hu, Z.; Yao, P. Novel interpenetrating polymer network sulfonated poly (phthalazinone ether sulfone ketone)/polyacrylic acid proton exchange membranes for fuel cell. *J. Membr. Sci.* **2007**, *295*, 80–87.

(72) Li, Z.; Friedrich, A.; Taubert, A. Gold Microcrystal Synthesis via Reduction of  $\text{HAuCl}_4$  by Cellulose in the Ionic Liquid 1-Butyl-3-methyl Imidazolium Chloride. *J. Mater. Chem.* **2008**, *24*, 1008–1014.

(73) Androne, D. A.; Dorohoi, D. O.; Timpu, D. Physical methods of identification of the feldspars from granitic pegmatites. *Rom. J. Phys.* **2008**, *53*, 279–286.

(74) Unuabonah, E. I.; Adebawale, K. O.; Olu-Owolabi, B. I.; Yang, L. Z.; Kong, L. X. Adsorption of Pb(II) and Cd(II) from aqueous solution onto sodium tetraborate-modified kaolinite clay: Equilibrium and thermodynamic studies. *Hydrometallurgy* **2008**, *93*, 1–9.

(75) Unuabonah, E. I.; Olu-Owolabi, B. I.; Adebawale, K. O.; Ofomaja, A. E. Adsorption of lead and cadmium ions from aqueous solutions by tripolyphosphate-impregnated kaolinite clay. *Colloids Surf. A: Physicochem. Eng. Aspects* **2007**, *292*, 202–211.

(76) Shukla, A.; Zhang, Y. H.; Dubey, P.; Margrave, J. L.; Shukla, S. S. The role of sawdust in the removal of unwanted materials from water. *J. Hazard. Mater.* **2002**, *95*, 132–152.

(77) El-Khaiary, M. I.; Malash, G. F. Common data analysis errors in batch adsorption Studies. *Hydrometallurgy* **2011**, *1–3*, 314–320.

(78) Lagergren, S. Zur theorie der sogenannten adsorption geloster stoffe. *Kungliga Svenska Vetenskapsakademiens. Handlingar* **1898**, *24*, 1–39.

(79) Ho, Y. S.; Ofomaja, A. E. Kinetics and thermodynamics of lead ion sorption on palm kernel fiber from aqueous solution. *Process Biochem.* **2005**, *40*, 3455–3461.

(80) Thirumal, J.; Kaliappan, S. Equilibrium, kinetic and thermodynamic behaviour of perchlorate adsorption onto the activated carbon. *Eur. J. Sci. Res.* **2011**, *64*, 365–376.

(81) Ho, Y. S. Citation reviews of Lagergren kinetic rate equation on adsorption reactions. *Scientometrics* **2004**, *59*, 171–177.

(82) Puls, W. R.; Bohn, H. L. Sorption of cadmium, nickel, and zinc by kaolinite and montmorillonite suspensions. *Soil Sci. Soc. Am. J.* **1988**, *52*, 1289–1292.

(83) Pearson, R. G. Hard and soft acids and bases. *J. Am. Chem. Soc.* **1963**, *85*, 3533–3539.

(84) Klopman, G. Chemical Reactivity and the Concept of Charge- and Frontier-Controlled Reactions. *J. Am. Chem. Soc.* **1968**, *90*, 223–234.

(85) Onal, Y.; Akmil-Basar, C.; Sarıcı-Ozdemir, C. Investigation kinetics mechanisms of adsorption malachite green onto activated carbon. *J. Hazard. Mater.* **2007**, *B146*, 149–203.